IJSGS

ISSN: 2488-9229
FEDERAL UNIVERSITY
GUSAU-NIGERIA

INTERNATIONAL JOURNAL OF SCIENCE FOR GLOBAL SUSTAINABILITY

Preparation, Characterization and In-vitro Drug Release Study of Methotrexate-Loaded Hydroxyapatite-Sodium Alginate Nanocomposite

*C. C. Onoyima[1], F.G Okibe[2], E.B Agbaji[2], V.O Ajibola[2]

[1]Department of Chemistry, Nigeria Police Academy, Wudil, Nigeria
[2]Department of Chemistry, Ahmadu Bello University, Zaria, Nigeria

*Corresponding author: krissonoss@yahoo.co.uk

Received: May, 2016 Accepted: August, 2016

Abstract

Controlled drug delivery systems reduce dose-dependent toxicity associated with potent drugs, including anticancer drugs. In this research, hydroxyapatite (HA) and hydroxyapatite-sodium alginate nanocomposites (HASA) were successfully prepared and characterized using Fourier Transform Infrared spectroscopy (FTIR) and Scanning Electron Microscopy (SEM). The FTIR result showed absorption peaks characteristics of pure hydroxyapatite (HA), and also confirmed chemical interaction between hydroxyapatite and sodium alginate in the formation of the composite. Image analysis revealed nano-sized hydroxyapatite and hydroxyapatite-sodium alginate nanocomposites with irregular morphologies. Particles sizes increased with the formation of the nanocomposites relative to pure hydroxyapatite, with no significant change in particles morphologies. Drug loading and in-vitro drug release study was carried out using synthetic body fluid as the release medium, at pH 7.4 and 37 ^{0}C and under perfect sink conditions. The result shows that drug loading is highest for pure hydroxyapatite and decreased with increasing quantity of sodium alginate. However, the release study revealed that HASA-5%wt and HASA-20%wt presented better release profiles than pure hydroxyapatite, while HASA-33%wt and HASA-50%wt have poor release profiles. This shows that Methotrexate-loaded hydroxyapatite-sodium alginate if prepared under optimal conditions is a potential carrier for effective delivery of Methotrexate.

Keywords: *Hydroxyapatite; Nanocomposites; Methotrexate; Drug-delivery; Sodium alginate.*

1.0 INTRODUCTION

Hydroxyapatite is a calcium phosphate salt. It is the main component of vertebrate hard tissues such as bone and teeth in the form of nanometer-sized needle-like crystals of approximately 5-20 nm width by 60 nm length (Ferraz *et al.*, 2004). In recent years synthetic nano-hydroxyapatite has been widely used in biomaterials such as drug delivery, orthopedic and dental applications. This is as a result of its excellent useful properties such as biocompatibility, bioactivity, osteo-conductivity, and is non-toxic, non-inflammatory, and non-immunogenic (Mateus *et al.*, 2008). Hydroxyapatite-polymer composites have attracted much attention since such composite lead to improved properties

(Khaled, *et al*., 2014) such as sustained drug delivery (Raj *et al.*, 2013)

Nanocomposite is a composition having dispersed material that has one or more dimensions, such as length, width, and thickness in the nanometer size range (Roul *et al*., 2013). The final properties of the nanocomposite are very often not a simple addition of the properties of the independent components, but a unique result from synergistic effect (Hood *et al*., 2014).

It has been shown that the drug loading efficiency and controlled release behavior can be enhanced because of the synergistic effect between biopolymer and inorganic materials (Devanand *et al*., 2011).

Methotrexate (4-amino-10-methylfolic acid) is a hydrophilic anticancer drug widely used for treatment of a number of diseases such as leukemia, lymphomas, osteosarcoma, and rheumatoid arthritis. (Nerves *et al*, 2009). However, despite its importance, its use is limited by dose-dependent toxicity ranging from malaise, esthenia, to gastrointestinal and hepatic toxicity, and pencytopenica which can be fatal (Khan *et al*., 2010). Methotrexate efficacy is also limited by its short plasma half life (Yousefi *et al*., 2010). This research investigates solution to these limitations, by synthesizing and characterizing a biocompatible and biodegradable material capable of loading and releasing Methotrexate in a controlled manner.

2.0 MATERIALS AND METHODS

2.1 Preparation of Hydroxyapatite/Sodium Alginate Nanocomposites

The in-situ preparation of hydroxyapatite in the presence of sodium alginate was done according to the method by Rajkumar *et al.* (2011**)** with some modifications. The moles of the calcium and phosphate precursors were chosen so as to maintain a Ca/P mole ratio of 1.67, the stoichiometric amount of hydroxyapatite **(**$Ca_{10}(PO_4)_6(OH)_2$). Disodium hydrogen phosphate solution (0.06M) was prepared in distilled water. The phosphate solution was added in drop-wise manner to a separately prepared sodium alginate solution while stirring vigorously. The mixture was added drop by drop to aqueous solution of calcium nitrate tetrahydrate ($Ca(NO_3)_2.4H_2O$) (0.1M) prepared earlier with continuous stirring for 24h**.** The pH was maintained at approximately 10.5 throughout the experiment using sodium hydroxide solution. The suspension was then stored for 24h at room temperature for aging, after which the precipitate was separated by centrifugation, and subsequently washed with distilled water three times. The resulting gel-like paste was dried at 60^0C for 24h and then grinded using agate mortar to obtain fine powders.

The same procedure was repeated using varying quantities of sodium alginate. Similarly, the pure nano-hydroxyapatite was prepared using the above method but without sodium alginate. The equation of hydroxyapatite formation is given below:

$10Ca(NO_3)_2 .4H_2O + 6(NH_4)_2HPO_4 + 8NH_4OH \rightarrow \mathbf{Ca_{10}(PO_4)_6(OH)_2} + 20NH_4NO_3 + 46H_2O$

2.2 Preparation of Drug-Loaded Hydroxyapatite and Drug-Loaded Sodium Alginate/Hydroxyapatite Nanocomposites

Drug loading was done according to the method by Devanand *et al*. (2011). In order to load the drugs on hydroxyapatite nanoparticles, the drug, Methotrexate (MTX) was dissolved in distilled water. The concentration of the Drug was kept constant (2 mg/ml). Hydroxyapatite and hydroxyapatite/sodium alginate nanocomposites were added to the drug solution and stirred using magnetic stirrer for 40 min. Then the solution was left undisturbed overnight. The suspension was then centrifuged (2000 rpm, 5 min) and the supernatant and precipitate were separated. The amount of drug loaded was determined by finding the difference in the concentrations in the aqueous solution before and after loading. The drug encapsulation efficiency (EE) of hydroxyapatite and the nanocomposites were evaluated by measuring the absorption of the supernatant at 419 nm using UV spectrophotometer.

The EE was calculated according to the following equation (Papadimitriou, *et al*., 2008):

$$E\,E = \frac{C_i - C_f}{C_i}$$

C_i represents the total concentration of drug; C_f is the concentration of free drug in the

supernatant. All measurements were performed in triplicate and the mean values reported

2.3 Material Characterizations

2.3.1 Fourier Transform Infrared Spectroscopy (FTIR)

FT-IR analysis was conducted to identify the functional groups of the samples. Infrared spectra in the wavenumber range of 650-4000 cm^{-1} were recorded with Cary 630 Agilent Fourier Transform infrared spectrometer. The analyses were carried out with 8 scans at 16 cm^{-1} resolution, applying transmittance method.

2.3.2 Scanning Electron Microscopy (SEM)

The hydroxyapatite and the composites containing different concentrations of sodium alginate were characterized using Scanning Electron Microscope (SEM). The powdered samples were placed on standard aluminum specimen mounts (pin type) with double-sided adhesive electrically conductive carbon tape. The specimen mounts were then coated with 60% Gold and 40% Palladium for 30 seconds with 45 mA current in a sputter coater. The coated samples were then observed on the SEM using an accelerating voltage of 20 kV at a tilt angle of 30^0.

2.3.3 Image Analysis

Image analysis of the particles was carried out using ImageJ software, developed at the National Institute of Health (NIH) (Schneider *et al*., 2012). The scale bar was used to convert the pixel unit of the image to nanometer units. The bandpass-filtered image was thresholded to set the lower and upper threshold values, segmenting the image into particles and background. The micrograph was then binarised using watershed segmentation. The 'set measurement' was used to select relevant parameters for measurement; and the analysis was limited to threshold area, excluding particles on edges and structures with aberrant morphology.

An image analysis system could describe non-spherical particles using the Feret diameter, perimeter, projected area, spherical equivalent diameter, circularity and aspect ratio (ISO 9276-6):

- Feret diameter; this is the longest distance between any two points along the particle boundary.
- Spherical equivalent diameter (SED), = $\sqrt{\frac{4A}{\pi}}$

Where A is the area of the particle. This is the diameter of a circle with the same area as the particle.

- Perimeter (P): = $\frac{\pi}{N}\sum_{N}^{\pi} l_{\alpha} dL$

This is the Cauchy-Crafton equation with l as the number of intercepts formed by a series of parallel lines, with spacing dL, exploring N directions from α to π.

- Circularity (C) = $\sqrt{\frac{4\pi A}{P^2}}$

Where A is the area and P the perimeter of the particle. The values range from 0 to 1, the closer it is to unity the more spherical the particles. In order words, the further away from a perfectly round and smooth circle that a particle becomes, the lower the circularity value.

- Aspect ratio (A.R) = $\frac{\text{minor axis}}{\text{major axis}}$

  A.R is a dimensionless quantity and has been scaled by ISO 9276-6 to always be in the range $0 \geq A.R \leq 1$. Symmetric particles have high aspect ratio.

2.4 In Vitro Drug Release Study

The *in vitro* drug release study was carried out following a method reported by Sivakumar and Panduranga-Rao, (2002). In order to determine the drug release profile, 100 mg of the drug loaded nanocomposite and drug loaded hydroxyapatite was introduced into a screw capped glass bottle containing 50 ml of synthetic body fluid (SBF) medium at 37°C and pH 7.4 under sterile conditions. 5 ml samples were withdrawn by a pipette at regular intervals and replaced immediately with 5 ml of fresh SBF medium, which was accounted for when calculating the amount of drug released. Drug concentration in the collected samples were

measured at 419 nm using UV-VIS Spectrophotometer.

3.0 RESULTS AND DISCUSION

3.1 Fourier Transform Infrared Spectroscopy (FTIR)

Figure 1 shows the FTIR spectra of pure hydroxyapatite (HA), sodium alginate (SA), Hydroxyapatite-Sodium alginate (HASA), Methotrexate-loaded hydroxyapatite (HA-MTX), and Methotrexate-loaded hydroxyapatite-sodium alginate (HASA-MTX). Characteristic bands for hydroxyapatite were observed. The band at 3384.4 cm^{-1} was due to O–H stretching vibration; the band at 1640 cm^{-1} attributed to O-H bending mode of absorbed water. This band has been previously reported for hydroxyapatite (Sanosh *et al*., 2009; Venkatesan *et al*, 2011). The most intense peak at 1021.3 cm^{-1} is due to asymmetric stretching of PO_4^{3-}, while the weak peak at 2012.8 cm^{-1} is due to its overtone and/or combination band which is in agreement with the values reported in literature (Pramanik *et al*., 2006; Rajkumar *et al*., 2010; Rajkumar *et al*., 2011). The observed bands at 1453.7 cm^{-1} and 1412.7 cm^{-1} are due to asymmetric stretching mode of CO_3^{2-}, while the band at 872.2 cm^{-1} resulted from bending mode of CO_3^{2-}. The presence of carbonate ions in apatite has been reported (Rajkumar *et al*., 2010; Tkalčec *et al*., 2014) and is believed to occur during the preparation of hydroxyapatite when CO_2 from the atmosphere reacts with hydroxyl ion and forms carbonate ions according to the equation below (Azami *et al*., 2010; Cunniffe *et al*., 2010; Anuar, *et al*., 2013):

$$CO_2 + 2OH^- \longrightarrow CO_3^{2-} + H_2O$$

Carbonate formation occurs in hydroxyapatite synthesized at low temperature, and is reduced after sintering at 800 ^{0}C (Alobeedallah, 2011). According to Sanosh *et al*., (2009), the presence of carbonate ions in hydroxyapatite is likely to improve its bioactivity. It increases the solubility of hydroxyapatite, and reduces its crystallite size.

Spectrum of sodium alginate exhibited bands which are in agreement with the reference data. These include bands at 3236.3 cm^{-1} attributed to O-H stretching mode, 2922.2 cm^{-1} due to C-H asymmetric stretching, 1297.1 cm^{-1} and 887 cm^{-1} due to C-H in-plane and out-of-plane bending respectively. The peaks at 1595.3 and 1405.2 are due to COO^- stretching vibrations, while peaks at 1103.3 cm^{-1} and 1025 cm^{-1} are due to C-O and C-O-C stretching vibrations. C-C stretching mode also absorbs here.

The formation of the composite was confirmed by the spectrum of HASA in figure 1. It was observed that the band at 3236.3 cm^{-1} in alginate shifted to 3220.4, while the bands at 1595.3cm^{-1} and 1405.2 cm^{-1} shifted to 1599.0 cm^{-1} and 1408.9 cm^{-1} respectively. As divalent metal ions replace sodium ions in the sodium alginate, the charge density, the radius and atomic weight of the cation are changed, creating a new environment around the carbonyl group, hence the observed peak shift (Azami *et al*., 2010). This also leads to the formation of new peak at 1341.8 cm^{-1}. It has been documented that formation of chemical bond between carbonyl group and divalent metal leads to a new peak around 1340 cm^{-1} (Kikuchi *et al*., 2004; Itoh *et al*., 2005; Azami *et al*., 2010).

Methotrexate (MTX), Methotrexate-loaded hydroxyapatite (HA-MTX) and Methotrexate-loaded hydroxyapatite-sodium alginate (HASA-MTX) exhibited similar bands at 3268.9 cm^{-1} assigned to O-H stretching vibration overlapped with N-H stretching mode; band at 1636.3 cm^{-1} assigned to N-H bending mode; 1036.2 cm^{-1} due to C-O stretch and PO_4^{3-} from hydroxyapatite. The bands around 2101cm^{-1} – 2106 cm^{-1} is probably as a result of overtone or combinational band. There was no evidence of chemical interaction between the drug and hydroxyapatite or the composites.

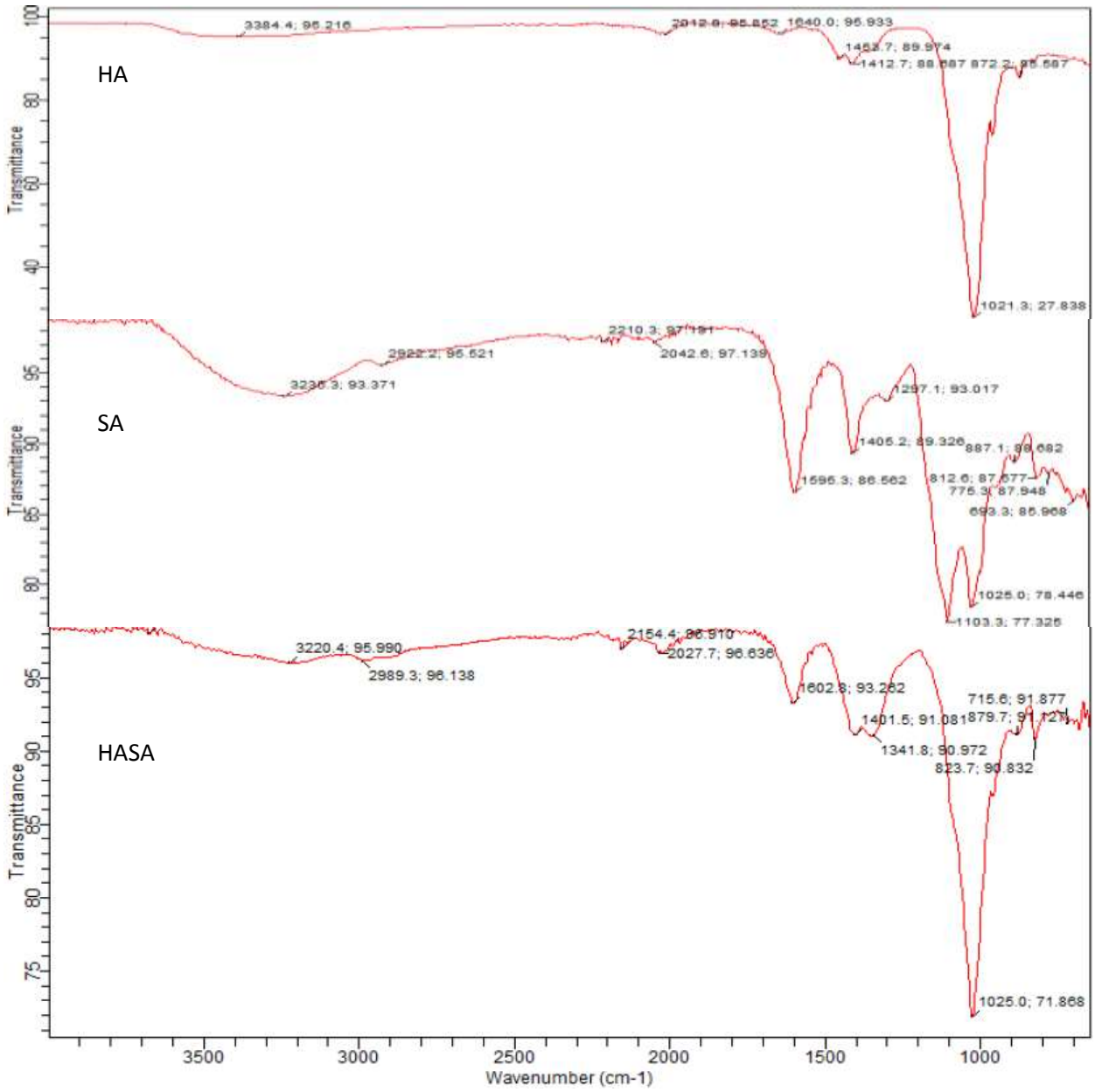

Figure 1: FTIR spectra of Hydroxyapatite (HA), Sodium alginate (SA), and hydroxyapatite-sodium alginate (HASA).

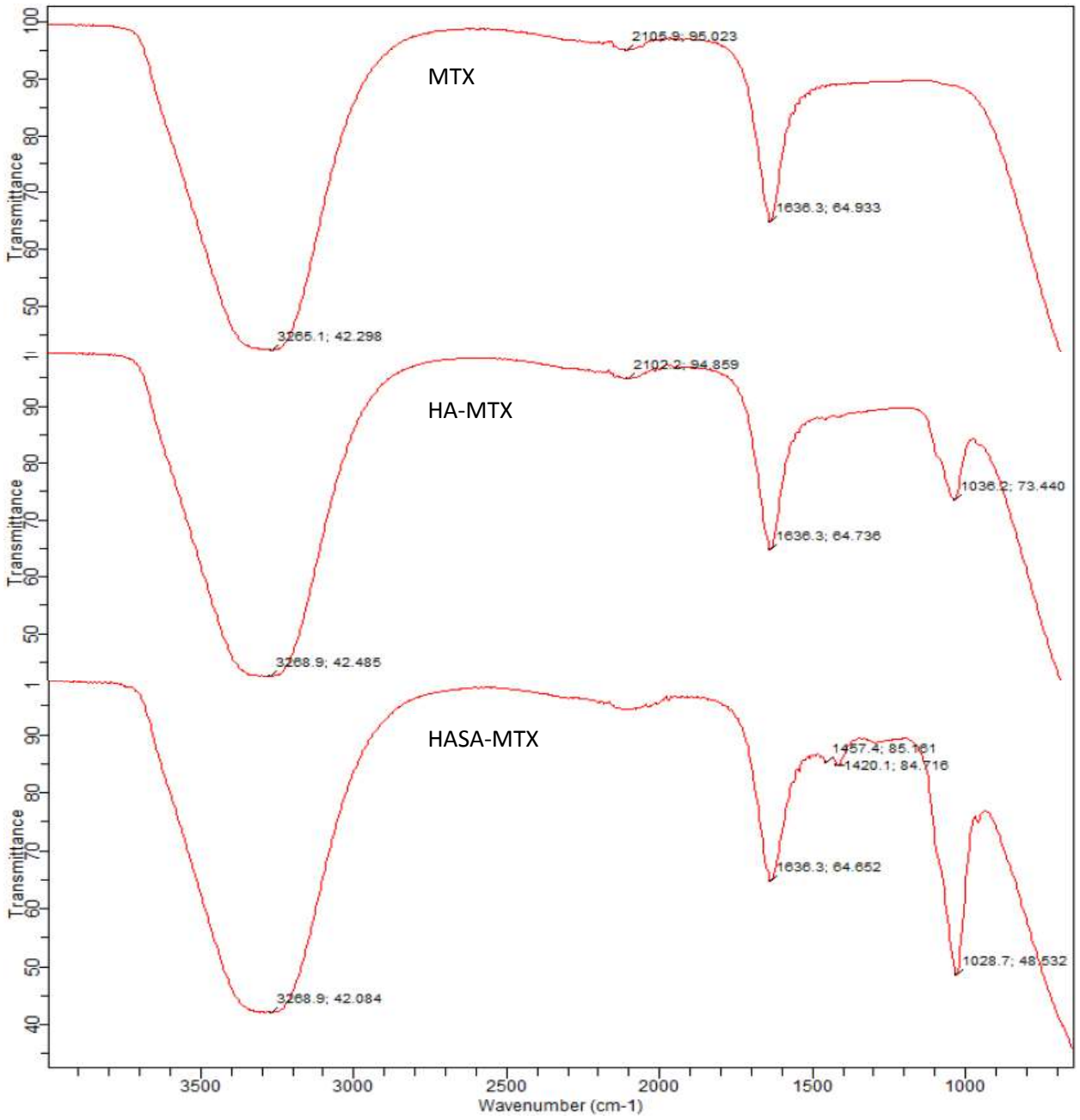

Figure 2: FTIR spectra of Methotrexate (MTX), Methotrexate-loaded hydroxyapatite (HA-MTX), and Methotrexate-loaded hydroxyapatite-sodium alginate (HASA-MTX).

3.2 Scanning Electron Microscopy

Figure 3 illustrates the scanning electron micrograph of hydroxyapatite (HA) and Hydroxyapatite-sodium alginate nanocomposite (HASA). In order to extract valuable information from the images, particle size and shape factors were measured using image analysis technique. Shape factors may dictate the behavior of a product or correlate to a response of interest (Olson, 2011). United State Pharmacopeia (USP) <776> Optical Microscopy (2011) also emphasized the need for shape factor determination, including information on the type of diameter measured for irregularly shaped particles.

The results of size and shape parameters of hydroxyapatite are presented in Table 1. Because the particles are irregularly shaped, two types of particle size measurements were used, the Spherical Equivalent Diameter, and the Feret Diameter. The Spherical Equivalent Diameter, also called the area equivalent diameter, or circular equivalent diameter, is defined as the diameter of a circle with the same area as the particle (Olson, 2011). Feret Diameter which is the longest distance between any two points along the particle boundary, tend to overestimate the particle size; hence spherical equivalent diameter is most widely cited. (Dune Sciences, 2011).

According to ISO 13322-2, it is wrong and misleading to report result of particles measurements using single value such as mean. A better approach is to report both a central point of the distribution along with one or more values (such as D10, D90 and standard deviation) to describe the width of the distribution. Table 1 shows that sizes of the hydroxyapatite particles range from 24.68 nm to 724.90 nm. 10% (D10) of the synthesized hydroxyapatite particles have diameter less than 46.16 nm; (In order words, 90% of the particles have sizes more than 46.16 nm); the sizes of 50% of the particles are below 85.50 nm; and only 10% of the particles have sizes above 280.89 nm. This result indicates that all the particles are within nanometer size range. This is particularly important for powders, suspensions and emulsion as particle size has great influence on their properties and behaviors. For example, the size and shape of powders influence flow and compactness properties. Larger, more spherical particles will typically flow more easily than smaller or low aspect ratio particles. Smaller particles dissolve more quickly and lead to higher suspension viscosities than larger ones (Horiba Scientific, 2014). The histogram of the particles size distribution of hydroxyapatite is displayed in figure 4.

The results from Table 1 also show that the particles are of irregular shapes. This can be seen from the results of the shape parameters such as aspect ratio and circularity.

As sodium alginate was added to form the nanocomposite, particle size increased with wider size distribution (Table 2). The range of the size (spherical equivalent diameter) is from 41.80 nm to 997.97 nm. However, the shape parameters, namely the aspect ratio (A.R) and the Circularity are similar to that of pure hydroxyapatite. The wide difference between the spherical equivalent diameter and the Feret diameter is a further evidence of irregularity of the particles' morphology. The more spherical the particles are, the closer the values of the two types of size.

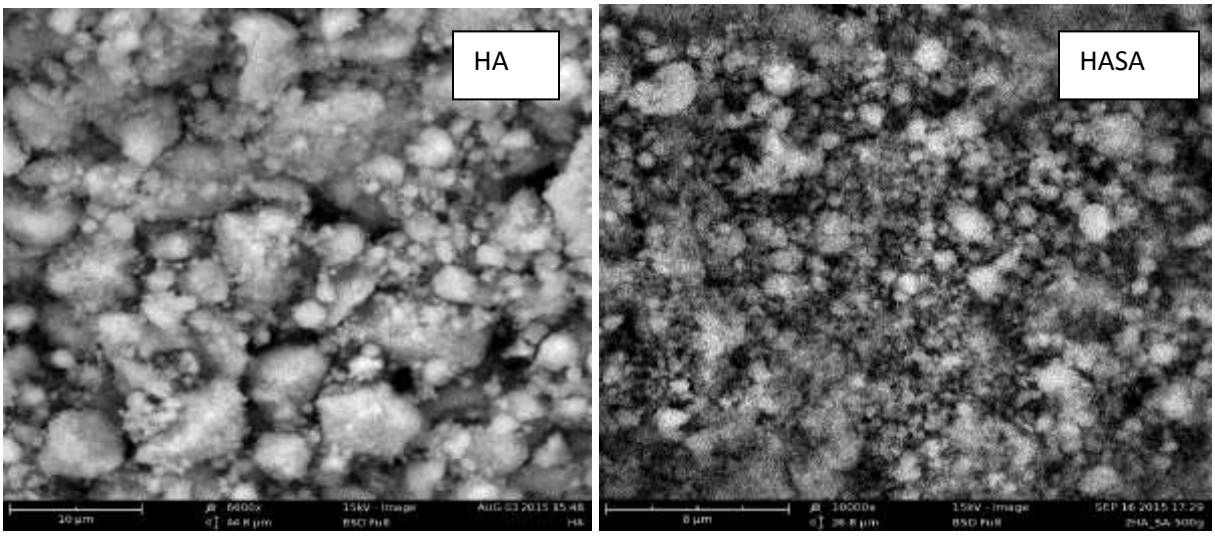

Figure 3: Scanning electron micrograph of hydroxyapatite (HA) and hydroxyapatite-sodium alginate nanocomposite (HASA).

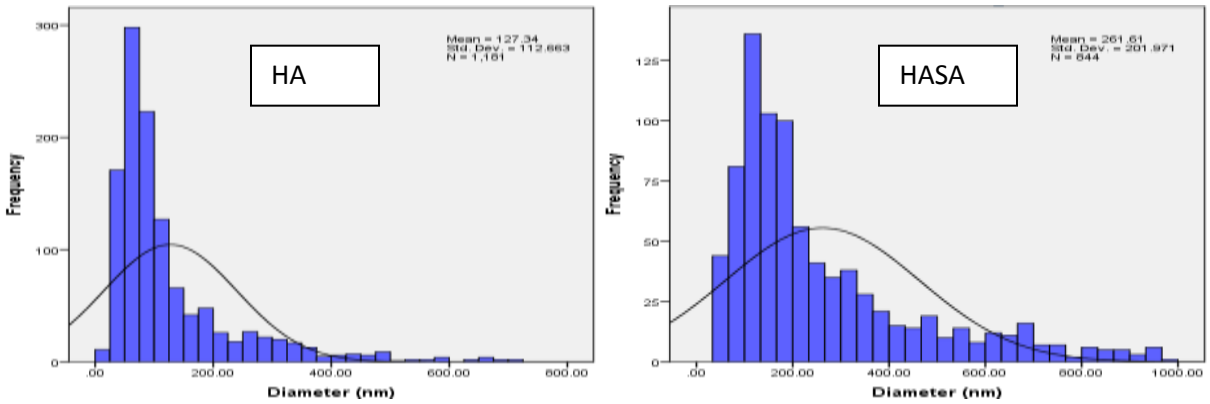

Figure 4: Particle size distribution of hydroxyapatite (HA) and hydroxyapatite-sodium alginate nanocomposite (HASA).

Table 1: Size and shape parameters of hydroxyapatite (HA)

Statistic	SED (nm)	F.D (nm)	A.R	Circularity	Perimeter (nm)
D10	46.18	69.12	0.3798	0.439	153.08
D50(Median)	85.50	132.12	0.5782	0.703	320.53
D90	280.89	405.91	0.8017	0.922	1258.71
Standard Error	3.2784	4.59	0.00465	0.00530	15.68
Mean	127.34	189.58	0.5860	0.692	531.66
Mode	57.89	69.16	0.5166	0.857	236.81
Standard Dev.	112.66	157.62	0.1599	0.1822	538.81
Kurtosis	6.29	6.12	-0.5472	-1.0219	6.36
Skewness	2.34	2.26	0.1850	-0.2282	2.38
Range	700.22	1071.81	0.7695	0.740	3258.78
Minimum	24.68	43.74	0.2305	0.248	87.48
Maximum	724.90	1115.54	1	0.988	3346.26
Count	1181	1181	1181	1181	1181

SED=Spherical equivalent diameter**, F.D** = Feret diameter**, A.R** = Aspect ratio

Table 2: Descriptive statistics of size and shape parameters of HASA

Statistic	SED (nm)	F.D (nm)	A.R	Circularity	Perimeter (nm)
D10	83.60	131.15	0.3895	0.4510	305.75
D50(Median)	184.59	282.50	0.6280	0.6715	719.61
D90	584.46	821.53	0.8270	0.9160	2672.32
Mean	261.61	379.50	0.6205	0.6790	1093.75
Standard Error	6.952	9.459	0.00563	0.00608	32.987
Mode	121.87	189.14	0.3333	0.9670	401.67
Standard Deviation	201.970	274.794	0.1634	0.1766	958.332
Kurtosis	1.6960	1.2662	-0.7369	-0.9843	2.2421
Skewness	1.5115	1.3766	-0.0823	-0.0316	1.6262
Range	956.17	1345.60	0.7629	0.8120	5022.43
Minimum	41.80	74.19	0.2370	0.1760	148.38
Maximum	997.97	1419.79	1	0.9880	5170.81
Count	844	844	844	844	844

SED=Spherical equivalent diameter, F.D = Feret diameter, A.R = Aspect ratio.

3.3 Drug Loading and Release Study

Figure 5 shows the result of Methotrexate loading in hydroxyapatite and hydroxyapatite-sodium alginate nanocomposites. The result shows that the amount of methotrexate loading depends on the quantity of hydroxyapatite relative to the sodium alginate. Methotrexate loading was highest in hydroxyapatite alone (35.24%), and decreased with increasing addition of sodium alginate as follows: HASA-5%wt (24.84%), HASA-20%wt (21.49%), HASA-33%wt (14.93%), HASA-50%wt (10.78%). From the FTIR study, it was observed that there was no chemical interaction between hydroxyapatite (HA) and methotrexate (MTX), therefore the higher drug loading in hydroxyapatite may be due to its higher porosity.

The release profiles of the drug-loaded hydroxyapatite and the drug-loaded hydroxyapatite-alginate nanocomposites using simulated body fluid as the release medium (SBF), at pH 7.4 and 37 ^{0}C are illustrated in figure 6. The release study was conducted for 23 hours. Hydroxyapatite released 83.76% of the loaded drug in 2 hours, while HASA-5%wt and HASA-20%wt released 89.08% and 83.56% of the drug respectively in 3 hours. For HASA-33%wt and HASA-50%wt formulations, there was no further release of the drug after the first sampling period as the percent cumulative decreased continuously. From this result, we can infer that addition of small amount of alginate up to 20%wt to hydroxyapatite extended the release of the drug for additional one hour, after which further addition reduced drug loading and increased burst release effect.

In order to further characterize the release profiles, profile comparison of the different formulations was carried out using DDSolver, an excel add-In. Pairwise procedure was followed and similarity factor (F_2) was chosen for the comparison. The results show that hydroxyapatite (HA) has a similar release profile with HASA-5%wt and HASA-20%wt with similarity factors (F_2) of 50.14 and 65.02 respectively (i.e HA vs HASA-5%wt and HA vs HASA-20%wt). On the other hand, hydroxyapatite did not exhibit similar release profile with HASA-33%wt and HASA-50%wt, as the similarity factors (F_2) are 36.58 and 33.35 respectively (note: two release profiles are similar if $50 \leq F_2 \leq 100$ (Zuo *et al*., 2014)).

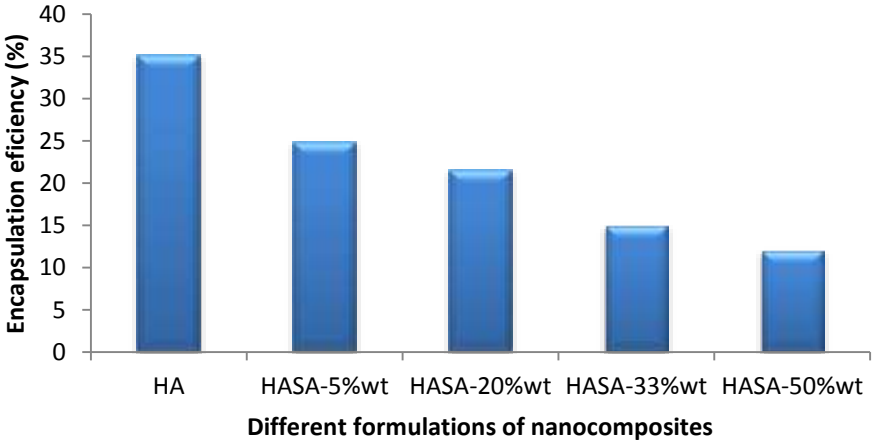

Figure 5: Drug encapsulation efficiency of hydroxyapatite and the nanocomposites.

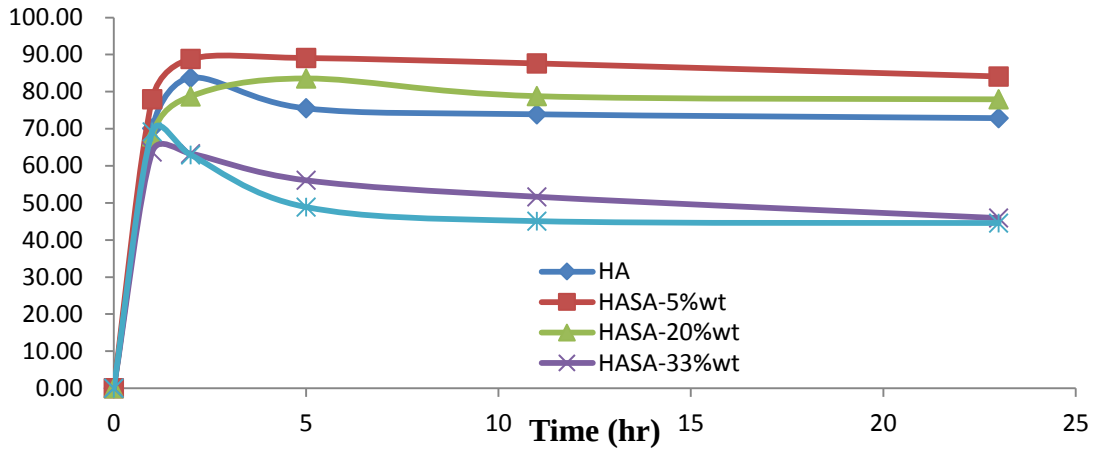

Figure 6: Drug release profiles of hydroxyapatite and the nanocomposites.

4.0 CONCLUSION

Hydroxyapatite-sodium alginate nanocomposites have been successfully synthesized and characterized. The FTIR results showed functional groups typical of pure hydroxyapatite, and also confirmed the formation of the composites. Image analysis classified the materials as non-spherical, irregular and of nano-size. The drug delivery ability of hydroxyapatite was observed to increase with the addition of little quantity of sodium alginate (up to 20% wt).

5.0 REFERENCES

Alobeedallah, H., Ellis, J.L., Rohanizadeh, M., Coster, H., and Dehghani, F. (2011). Preparation of Nanostructured Hydroxyapatite in Organic Solvents for Clinical Applications. *Trends Biomater. Artif. Organs, 25(1), 12-19.*

Anuar, A., Salimi, M.N., Daud, M.Z., and Yee, F.Y. (2013). Characterizations of hydroxyapatite (HAp) nanoparticles produced by sol-gel method. *Advances in Environmental Biology*, x(x), 3587-3590.

Azami, M., Samadikuchaksaraei, A., and Poursamar, S. A. (2010). Synthesis and characterization of a laminated hydroxyapatite/gelatin nanocomposite scaffold with controlled pore structure for bone tissue engineering. *International Journal of Artif. Organs*, 33 (2), 86-95.

Cunniffe, G.M., O'Brien, F.J., Partap, S., Levingstone, T.J., Stanton, and K.T., Dickson, G.R. (2010). The synthesis and characterisation of nanophase hydroxyapatite using a novel disperant-aided precipitation method.*Journal of Biomedical Materials Research. Part A.* 95(4):1142-9.

Devanand, V.G., Ramasamy, S., Ramakrishnan, V., and Kumar, J. (2011). Hydroxyapatite – Alginate nanocomposite as drug delivery matrix for sustained release of ciprofloxacin. *Journal of Biomedical Nanotechnology*, 7, 1- 9.

Ferraz, M.P., Monteiro, F.J., and Manuel, M. (2004). Hydroxyapatite nanoparticles: A review of preparation methodologies. *Journal of Applied Biomaterials & Biomechanics*, 2, 74-80.

Horiba Scientific. (2014). A guide book to particle size analysis. Horiba Instruments, Inc. Irvine, CA 92618 USA. www.horiba.com/us/particle

ISO 13322-2. Particle size analysis-Image analysis method-Part 2: Dynamic image analysis methods.

ISO, *ISO 9276-6: (2008*). Representation of results of particle size analysis–Part 6: Descriptive and quantitative representation of particle shape and morphology.

Khaled, R.M., Hanan, H.B., and Zenab, M. E. (2014). In-vitro study of nano-hyroxyapatite/gelatine-chitosan composites for bio-application. *Journal of Advanced Research*, 5, 201 – 208.

Itoh, S., Kikuchi, M., and Koyama, Y. (2005). Development of a novel biomaterial, hydroxyapatite/collagen (HAp/Col) composite for medical use. *Biomedical and Material Engineering*, 15, 29-41.

Khan, M.S., Priyadarshini, M., Sumbul, S., and Bano, B. (2010). Methotrexate binding causes structural and functional changes in lung cystatin. *Acta Biochimica Polonica*, 57 (4), 499-503.

Hood, M.A., Mari, M., and Muñoz-Espí, R. (2014). Synthetic Strategies in the Preparation of Polymer/Inorganic Hybrid Nanoparticles. *Materials*, *7*, 4057-4087.

Kikuchi, M., Matsumoto, H.N., Yamada, T., Koyama, Y., Takakuda, K., and Tanaka, J. (2004). Glutaraldehyde cross-linked hydroxyapatite/collagen self-organized nanocomposites. Biomaterials, 25, 63-9.

Mateus, A.Y, Barrias, C.C, Ribeiro, C., Ferraz, M.P., and Monteiro, F.J. (2008). Comparative study of nanohydroxy apatite microspheres for medical applications. *Journal of Biomed Material Resource A*, 86, 483 – 93.

Neves, C., Jorge, R., and Barcelos, A. (2009). The network of Methotrexate toxicity. *Acta Reumatol Port* 34, 11–34.

Olson, E. (2011). Particle shape factors and their use in image analysis – part 1: Theory. *Journal of GXP Compliance*, 15 (3), 85 – 96.

Papadimitriou, S., Bikiaris, D., Avgoustakis, K., Karavas, E., and Georgarakis, M. (2008). Chitosan nanoparticles loaded with dorzolamide and pramipexole. *Carbohydrate Polymers*, 73, 44–54.

Pramanik, N., Bhargava, P., Alam, S., and Pramanik, P. (2006). Processing and properties of nano- and macro-hydroxyapatite/poly (ethyleneco-acrylic acid) composites. *Polymer Composites*, 27, 633-641.

Raj, M.S., Arkin, V.H., Adalarasu, J., and Jagannath M. (2013). Nanocomposites Based on Polymer and Hydroxyapatite for Drug Delivery Application. *Indian Journal of Science and Technology*, 6(5S), 4653 – 4658.

Rajkumar, M., Sundaram, N.M., and Rajendran V. (2010). In-situ preparation of hydroxyapatite nanorod embedded poly (vinyl alcohol) composite and its characterization. *International Journal of Engineering Science and Technology*, 2(6), 2437 – 2444.

Rajkumar, M., Meenakshisundaram, N., and Rajendran, V. (2011). Development of nanocomposites based on hydroxyapatite/sodium alginate: Synthesis and characterization. *Material Characterization*, 62, 469-479.

Roul, J., Mohapatra, R., and Sahoo, S.K. (2013). Preparation, characterization and drug delivery behavior of novel biopolymer/ hydroxyapatite nanocomposite beads. *Asian Journal of Biomedical and Pharmaceutical Sciences*, 3(24), 33-38.

Sanosh, K.P., Chu, M., Balakrishnan, A., Kim, T.M., and Cho, S. (2009). Preparation and characterization of nano hydroxyapatite powder using sol–gel technique. *Bulletin of Material Science*, 32(5), 465–470.

Schneider, C.A., Rasband, W.S., and Eliceiri, K.W. (2012). NIH Image to ImageJ: 25 years of image analysis. Nature Methods, 9 (7), 671–675. doi:10.1038/nmeth.2089

Sivakumar, M., and Panduranga-Rao, K. (2002). Preparation, characterization and in vitro release of gentamicin from coralline hydroxyapatite–gelatin composite microspheres. Biomaterials 23, 3175–3181.

Tkalčec, E., Popović, J., Orlić, S., Milardović, S., and Ivanković, H. (2014). Hydrothermal synthesis and thermal evolution of carbonate fluorhydroxyapatite scaffold from cuttlefish bones. Materials Science and Engineering C, 42, 578–586. http://dx.doi.org/10.1016/j.msec.2014.05.079

USP, United States Pharmacopeia, <776> Optical Microscopy, USP34-NF29, 2011.

Venkatesan, P., Puvvada, N., Dash, R., Kumar, B.N., Devanand, S., Azab, B., Pathak, A., Kundu, S.C., Fisher, P.B., and Mandal, M. (2011). The potential of celecoxib-loaded hydroxyapatite-chitosan nanocomposite for the treatment of colon cancer. Biomaterial, 32, 3794 – 3806.

Yousefi, G., Foroutan, S.M., Zarghi, A., and Shafaati, A. (2010). Synthesis and Characterization of Methotrexate Polyethylene Glycol Esters as a Drug Delivery System. *Chemical and Pharmaceutical Bulletin*, 58(2), 147-53.

Zuo, J., Gao, Y., Bou-Chacra, N., and Löbenberg, R. (2014). Evaluation of DDsolver software application. *BioMed Research Internationl*, 2014, Article ID 204925. http://dx.doi.org/10.1155/2014/204925.